

Bootstrapping under constraint for the assessment of group behavior in human contact networks

Nicolas Tremblay,^{1,*} Alain Barrat,^{2,3,4} Cary Forest,⁵ Mark Nornberg,⁵ Jean-François Pinton,¹ and Pierre Borgnat¹

¹*Physics Laboratory, ENS Lyon, Université de Lyon, CNRS UMR 5672, Lyon, France*

²*Aix Marseille Université, CNRS, CPT, UMR 7332, 13288 Marseille, France*

³*Université de Toulon, CNRS, CPT, UMR 7332, 83957 La Garde, France*

⁴*Data Science Laboratory, Institute for Scientific Interchange (ISI) Foundation, Torino, Italy*

⁵*University of Wisconsin, Physics Department, Madison, USA*

(Dated: December 17, 2012)

The increasing availability of time – and space – resolved data describing human activities and interactions gives insights into both static and dynamic properties of human behavior. In practice, nevertheless, real-world datasets can often be considered as only one realisation of a particular event. This highlights a key issue in social network analysis: the statistical significance of estimated properties. In this context, we focus here on the assessment of quantitative features of specific subset of nodes in empirical networks. We present a resampling method based on bootstrapping groups of nodes under constraints within the empirical network. The method enables us to define confidence intervals for various Null Hypotheses concerning relevant properties of the subset of nodes under consideration, in order to characterize its behavior as “normal” or not. We apply this method to a high resolution dataset describing the face-to-face proximity of individuals during two co-located scientific conferences. As a case study, we show how to probe whether co-locating the two conferences succeeded in bringing together the two corresponding scientific communities.

Keywords: Complex System, Social Network, Graph Resampling, Bootstrap

* Corresponding author: `firstname.lastname AT ens-lyon DOT fr`

I. INTRODUCTION

High resolution measurements of face-to-face interactions between individuals in different social gatherings – such as scientific conferences, museums, schools, or hospitals – were made possible in the recent years by the use of wearable sensors, using bluetooth, wireless or RFID (Radio Frequency IDentification) technology. These new data paved the way to many empirical investigations [1–4] of human contacts, both from a static (e.g., existence of communities, clustering, heterogeneities in the number of contacts...) and dynamic (distribution of the durations of contacts, of the time between contacts, or of the lifetime of groups of different sizes...) points of view.

A major issue regarding the analysis of these datasets is that each represents a single realisation of a particular event: in contrast to the study of ensembles of random networks, it is not possible to generate multiple realizations of the event. Associating a statistical confidence to any measured property of these datasets is thus a challenging issue. In this context, various resampling methods have been proposed in the case of networks, in particular with the aim to assess the statistical significance of the empirical graph topology, for instance for phylogenetic trees [5] or bayesian-induced networks [6]. Another application concerns the significance of community structures [7, 8] in networks. In the present article, we do not address the significance of the empirical graph structure, that we consider as a fixed input, and we therefore do not try to generate resampled versions of the empirical graph as a whole. We focus instead on the statistical significance of features characterizing specific groups of nodes within the graph.

Two data-driven methods have been widely used in the general case to obtain confidence intervals for measurable features: the jackknife and bootstrapping [9, 10]. Both are based on drawing random samples from the unique original data recorded in an observation. Transposing the classical bootstrap approach to the case of data represented by graphs is however not straightforward; only a few works have considered resampling methods for graphs, in specific situations [11, 12]. In this paper, we focus on features of groups of nodes, and we formulate a bootstrap protocol: we consider resampled versions of the group of interest within the graph, and compare the studied group with its resampled versions. This enables us to define statistical significance by comparing the features measured in the real data and the ones measured in the random pseudosamples found under adequately chosen constraints.

Amongst other objectives, the proposed method gives estimates of the deviation of the behavior of a given group of nodes from a “normal” behavior (i.e., a Null Hypothesis for a statistical test) defined by the constrained random pseudosamples, enabling us to assess whether this given group’s behavior is normal or anomalous.

In order to illustrate the possibilities offered by this new resampling method, we apply it to the case study of a dataset describing the face-to-face interactions of individuals collected in two co-located conferences involving two distinct scientific communities: we will show how our method allows us to assess to what extent both communities mix together. Moreover, we test the performance of our method in a well-controlled tunable setting. To this aim, we generalize the Chung-Lu model of random graphs [13] to weighted networks, and we show how the bootstrapping method is able to assess whether groups of nodes in such networks are normal, anomalous and/or possibly rare.

The paper is structured in the following way. Section II presents the data and some of its general properties. We introduce in Section III the resampling method and we apply it to the data in Section IV. Finally, the weighted Chung-Lu graphs are introduced as benchmarks in Section V and the performance of the method is assessed on this model of complex network. We conclude in Section VI.

II. PRESENTATION OF THE DATASET OF TWO CO-LOCATED CONFERENCES

A. Data and pre-processing

We consider a dataset describing the face-to-face proximity of individuals collected in Salt Lake City (SLC) in November 2011 during two co-located scientific conferences lasting five days. These conferences were jointly organised by the DPP (Department of Plasma Physics) of the American Physical Society and the GEC (Gaseous Electronics Conference) in an attempt to bring together

both communities – mainly academic researchers and engineers respectively. The face-to-face proximity of the participants was measured using the SocioPatterns sensing infrastructure [1, 14] based on unobstrusive active RFID tags that can be embedded in conference badges. Two tags exchange radio packets only if the individuals wearing them face each other (the human body acts as a shield at this frequency and power) within a distance of 1 to 1.5 meters. The detected proximity relations are reported by the tags to RFID readers installed in the environment. At the end of the conference, the raw data consists of a log of all the recorded contacts. The log is a sequence of lines (t, r, i, j) where t is the time at which reader r received the information that the individuals wearing tags i and j were in close face-to-face proximity (“in contact”). Given the operating parameters of the tags, proximity of two individuals wearing the RFID badges can be assessed with a probability in excess of 99% over an interval of 20 seconds [1], which is a fine enough time scale to resolve human mobility and proximity at social gatherings. We therefore aggregate the raw data over time windows of 20 seconds: we partition the five days of data gathering into 20 second periods, and we associate to each of these periods t the adjacency matrix A^t representing the aggregated graph over the 20 seconds: $A_{ij}^t = 1$ if and only if vertices i and j have exchanged at least one radio packet during the time window t , otherwise $A_{ij}^t = 0$.

Overall, the data define a temporal contact network in which nodes represent individuals, and a link between two nodes at time t denotes the fact that the corresponding individuals are in face-to-face proximity. The temporal network can moreover be aggregated over the total duration of the conference, defining a weighted contact network where each node is an individual and where the weight of a link between two individuals gives the cumulated time they have spent in face-to-face interaction during the conference.

B. Distributions of contact durations

We first compare briefly the gathered data with other datasets collected in similar contexts using the same infrastructure. We define a contact between two tags i and j as an unbroken subsequence of 1’s within the sequence $\{A_{ij}^t\}$. Its duration is the length of this subsequence. Table II C presents basic statistics of the present data, together with the ones of data collected during the 2009 ACM HyperText conference (HT09) [15] and during a congress of the *Société Française d’Hygiène Hospitalière* (SFHH) [1]. Note that the sum of the total number of contacts (and the total time of contact) within DPP and within GEC does not exactly account for the interactions for the conference taken as a whole (ALL), due to the interactions between DPP and GEC. The SLC data contain a relatively small number of contacts, in comparison with the other conferences, taking into account the number of participants and the duration: this is due to the small sampling rate of the total population of the SLC conferences. The distribution of the duration of contacts are however very similar in the three contexts, displaying broad shapes with no typical scale, as shown in Fig. 1.a. Other statistical properties of the contact networks, such as the distribution of degrees, of the inter-contact times or of the weights of the links, also display a very similar behavior in these three contexts (see Appendix). This confirms the robustness of the main statistical properties of the networks of face-to-face contacts between individuals observed in previous works [2, 3, 15].

In the present dataset, we can distinguish three categories of contacts: within DPP, within GEC, and between both communities. Figure 1.b shows that even though the number of contacts is much larger within DPP than within GEC (see Table II C), the corresponding duration distributions collapse remarkably well upon one another. Hence, we do not observe any difference in the statistical behavior of the three categories of contacts. Let us also note that we are not interested here in modeling these distributions (for instance by power-law or log-normal functional forms), as the method we will use is data-driven. It is however of interest to remark that the broad shape of the distributions implies that parametric statistical method would be hard to implement, and that data-driven statistical methods are expected to be more adequate.

C. Distributions of the durations of contacts taking place in different places

The conference venue is spatially heterogeneous, with in particular three broadly defined areas: *the GEC Area* where the GEC registration and coffee breaks took place; *the Poster Hall*, where the

	HTT09	SFHH	SLC		
			GEC	DPP	ALL
# tags	113	418	39	281	320
sample rate	75%	33%	12%	16%	15%
# days	2	2	5		
# contacts	9582	27434	1189	21519	23920
Tot. time of contact (hours)	102	414	18	306	339

TABLE I. Basic statistics concerning the datasets collected in three different scientific conferences.

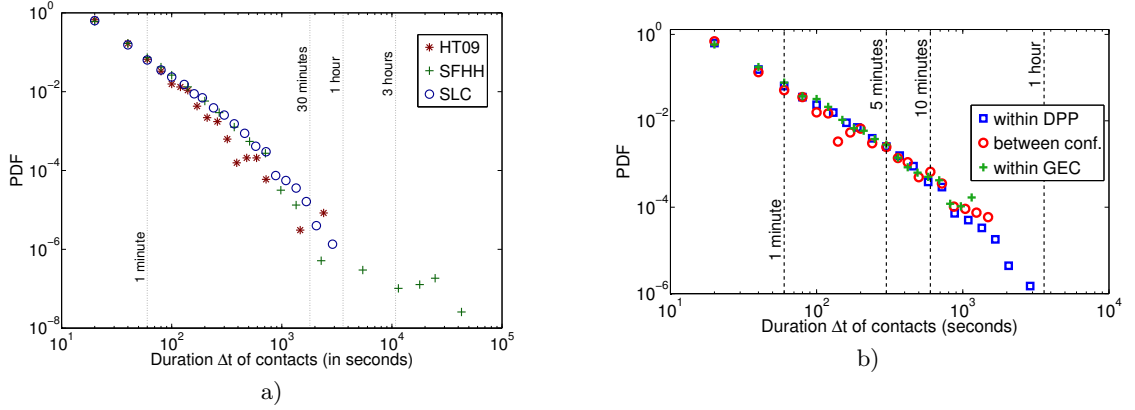


FIG. 1. a) Comparison of the distribution of the durations of contacts for three different datasets. b) Cumulative distributions of the durations of contacts within the DPP conference, within the GEC conference and between both conferences of the SLC experiment.

poster sessions of both conferences took place; and *the Rest*, which includes the DPP registration desk, two coffee break areas, and corridors linking different parts of the building. The GEC Area was situated 500 meters from the Poster Hall (maps are shown in the Appendix). It therefore took time and energy to walk from one area to another, not helping interactions between both communities. As the measuring infrastructure allows us to identify the area in which each reported contact took place, it is interesting to investigate if differences exist between the three types of contacts defined above when the spatial information is taken into account.

To this aim, we show in Fig. 2 the histograms of contact durations broken down by category of contact and area. For the DPP contacts (figure on the left), the distributions measured in the various areas have similar shapes, and the differences comes from the overall number of contacts measured in each area (as members of the DPP did not go much to the GEC area). On the other hand, for the contacts between both communities (figure in the middle) and for the GEC contacts (figure on the right), different slopes are observed depending on the area of interest. Broader distributions are obtained in the Poster Hall, in particular for the contacts between GEC and DPP attendees: the Poster Hall was therefore a more favorable setting for long cross-community contacts, as could indeed be expected.

III. BOOTSTRAPPING AND STATISTICAL TEST FOR COMPLEX NETWORKS

As discussed in the Introduction, our main objective is to provide statistical confidence on the measurements of properties of subsets of nodes in networks. To this aim, a standard way is to formulate a Null Hypothesis for the normal behavior of a group, and to perform a statistical test to decide whether or not to reject this Null Hypothesis. In this section, we will propose a series of statistical tests in the context of weighted networks using a specific resampling method based on bootstrapping constrained groups in the network.

We recall that bootstrapping [10] creates new random pseudosamples by using only one empirical

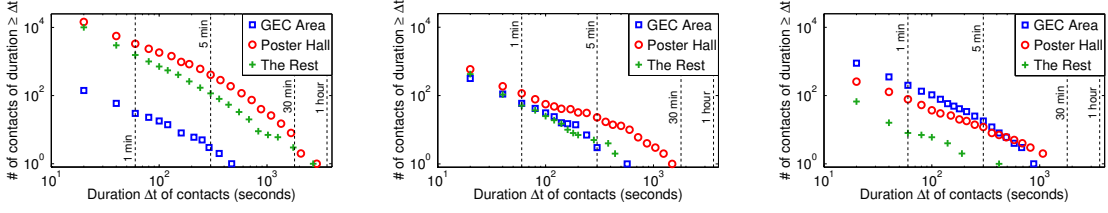


FIG. 2. Cumulative histograms of the durations of contacts in the three different areas within the SLC conference. Results for: (left) contacts within the DPP community, (middle) contacts between communities and (right) contacts within the GEC community.

observation of the data. The main advantage of using a bootstrap-inspired technique is that it does not require any supplementary information than the network itself: it is data-driven. Moreover, unlike other data-driven resampling methods such as the jackknife, it is possible to adapt the size of the drawn samples to the size of what is studied. Consequently, bootstrapping methods remain adequate even if the size of the groups that are studied has an impact on the estimated features.

An important issue when assessing significance of some features of a specific group in a network is that neither the nodes nor the links are independent from each other. This is reminiscent to the issue of creating correlated bootstraps in block bootstrapping [16, 17]. We will discuss this analogy in Section IV E. In order to use bootstrapping, it is required to propose a specific sampling method to draw replicates of groups with relevant properties. The method we propose is composed of two steps: 1) we decide on a specific scheme to draw groups that correspond to a proposed Null Hypothesis by imposing constraints on the extracted groups; 2) we then build a bootstrap set of many such groups, by randomly sampling them independently and with replacement, as in classical bootstrapping. Combining these two steps, we are then able to propose a bootstrap test to decide whether the specific group of interest is compatible with the proposed Null Hypothesis. We detail the proposed method in the next paragraphs.

A. Relevant observable features for groups in complex networks

Let $\mathcal{G} = (\mathcal{V}, \mathcal{E})$ be the graph representation of the studied complex network, with \mathcal{V} its set of nodes and \mathcal{E} its set of edges. We call $X^0 \subset \mathcal{V}$ the chosen subset of nodes whose behavior we compare to the behavior of “normal” groups, obtained as random bootstrap samples satisfying given constraints as explained above. Let us call $R^0 \subset \mathcal{V}$ the remaining nodes of the network that are not in X^0 .

We quantify X^0 ’s “behavior” by looking at several observable features that are representative of how the group is structured. In the context of social networks, relevant features are the ones that quantify whether there are strong contacts inside the group, possibly stronger than with other nodes. We choose here to use the following seven observable features (generically referred to as Z in the following), in addition to the cardinality M of the group X^0 :

- N_{XX}^0 the total number of links of \mathcal{E} between nodes of X^0 ;
- N_{RR}^0 the total number of links of \mathcal{E} between nodes of R^0 ;
- N_{XR}^0 the total number of links of \mathcal{E} connecting the two groups of nodes;
- T_{XX}^0 the total weight of links of \mathcal{E} between nodes of X^0 ;
- T_{RR}^0 the total weight of links of \mathcal{E} between nodes of R^0 ;
- T_{XR}^0 the total weight of the links connecting the two groups.
- Q_X^0 the modularity computed when partitioning the nodes of \mathcal{G} in two groups X^0 and R^0 .

In our case study, N_{XX} corresponds to the number of pairs of participants within the group X that have interacted at least once during the conference, and T_{XX} corresponds to the total time of contact between participants within the group X . We recall that the modularity is defined by [18]:

$Q = \frac{1}{2N} \sum_{i \in \mathcal{V}, j \in \mathcal{V}} \left[A_{ij} - \frac{k_i k_j}{2N} \right] \delta(c_i, c_j)$, where A is the weighted adjacency matrix, $k_i = \sum_{j \in \mathcal{V}} A_{ij}$ is the strength of node i , $N = \frac{1}{2} \sum_{i \in \mathcal{V}, j \in \mathcal{V}} A_{ij}$ is the total number of links, and c_i is the label of the group of node i (1 or 2 here as there are 2 groups), so that $\delta(c_i, c_j) = 1$ if nodes i and j are in the same group, and 0 otherwise. In this case of a partition in two groups, the modularity is a scalar between -0.5 and 0.5 and measures how well the partition separates the network into distinct communities (a value close enough to 0.5 denotes two strong communities).

The chosen observables are not fully independent and one might question why we consider so many. One of the most widely used observables regarding the behavior of a group in a network is the modularity [18]; however, modularity is neither a sufficient nor a unique way to discriminate between different types of behaviors. Two groups may have the same modularity but for very different reasons. By adding the six other observables that are admittedly not totally independent from the modularity, we accept some level of redundancy in the information we gather in order to yield a more complete and discriminative description of groups.

Depending on the specific issue addressed and of the nature of the complex network at hand, other observable features could be considered as relevant to describe the behavior of a group. We are here guided by the case study consisting in networks of face-to-face contacts between individuals, but we emphasize that the proposed procedure of bootstrap under constraints is directly usable in other contexts.

B. Protocol of bootstrapping for statistical test about a group in a network

The backbone of the developed method is the following.

1. First, we formulate a Null Hypothesis regarding the behavior of X^0 as being “normal” given a set of constraints on the group. This Null Hypothesis is converted in a specific set of constraints on the type of groups that should be in the bootstrap set. More specifically, these constraints define accepted values for the observable features of the bootstrap samples.
2. Second, we create a bootstrap set of N_B such groups by sampling from the data groups of nodes satisfying the constraints of the Null Hypothesis; we use X as a generic notation for the bootstrap samples. We recall that bootstrapping corresponds to taking these sample graphs with replacement.
3. For large enough N_B , we estimate the behavior of the graphs in the bootstrap set by estimating the mean and the variance of the various features. Estimation of this mean and variance for the Null Hypothesis is in essence fully data-driven and it defines a “normal behavior” for groups under this particular Null Hypothesis (i.e., under this particular set of constraints).
4. We compare the behavior of X^0 to this “normal behavior”, so as to decide whether or not we can reject the Null Hypothesis. If there is a significant deviation between the observed behavior of X^0 and the statistical behavior of the bootstrap samples, the Hypothesis is rejected for X^0 . In this case, one may compute a divergence measurement that evaluates to what extent X^0 deviates from the bootstrap samples and this measure will quantify the level of confidence with which the Null Hypothesis is rejected. To this aim, we will define in Section III C a suitable divergence d .

An important technical point is that the sampling method should allow us to draw sets of nodes that satisfy the chosen constraints. The simplest constraint is the cardinality constraint: we constrain the bootstrap samples’ size to match X^0 ’s. This constraint is trivially achieved: for each bootstrap sample, we randomly add nodes to it until its size reaches X^0 ’s.

Other Null Hypotheses lead us to impose stronger constraints by requiring one (or more) observables to be the same in X as in X^0 . For example, a stronger constraint is the “same N_{XX} ” constraint, in which we impose that each bootstrap sample has the same number of nodes and the same number of internal links than X^0 . In order to find bootstrap samples satisfying constraints such as this one, we use a simulated annealing algorithm [19] as follows.

We start with a random set of nodes X , with the same cardinality as X^0 , and we define the cost C of X as the difference between its number of internal links and the one of X^0 . We use an auxiliary “temperature” T that starts at high values. At each step of the simulated annealing

procedure, we keep some of the nodes of X and change the rest (the higher is T , the more nodes we attempt to change). If the cost C' of the new group is lower than C , we accept the change. If instead $C' > C$, we accept the change with probability $p \propto \exp\left(\frac{C-C'}{T}\right)$. When the cost does not decrease during several attempts, we lower the auxiliary temperature and start the whole process again. We stop the algorithm as soon as X satisfies the constraint (as soon as $C = 0$). We repeat this process N_B times to obtain the whole bootstrap set corresponding to this constraint.

C. Normalization of features and choice of the divergence d

Each observable Z is normalized into a dimensionless quantity z known as the “Z-score”: $z = \frac{Z - \bar{Z}^*}{\sigma_Z^*}$ where \bar{Z}^* is the expected value and σ_Z^* the standard deviation of the observable Z in a random graph with same weight sequence. To construct these random graphs, let us consider the full weight sequence (including the zero weights, corresponding to absent links), and randomly re-allocate the weights within the ensemble of possible links (i.e., pairs of nodes). This randomizes the degree of the nodes as well as their strengths (the strength is defined as the sum of the weights of the links of a node) and the local topological structures, and only preserves the weight sequence. This normalization may seem arbitrary, but this mode of representation is chosen for its clarity (we can plot all 7 observables on the same figure) and because it removes the effects due to the scale of the groups allowing us to compare the results between different groups. Indeed, \bar{Z}^* and σ_Z^* depend on X^0 's cardinality M . For each normalized observable z , we compute the mean \bar{z}^b and the standard deviation σ_z^b of the ensemble of bootstrap samples.

As mentioned above, we also need to define a divergence d quantifying if X^0 is far from the bootstrap set or not. For each observable feature Z , we define a divergence d_z as the distance between z^{X^0} , the actual measured value for X^0 , and the interval $[\bar{z}^b - 3\sigma_z^b, \bar{z}^b + 3\sigma_z^b]$ ($d_z = 0$ if z^{X^0} is in the interval). This interval would have the meaning of an acceptance interval for the Null Hypothesis if the observables were Gaussian. Indeed, more than 99% of the realisations of Gaussian random variable lie within 3 standard deviations of the mean [20]. The distance to the interval measures thus the deviation of the observed value for X^0 from the core of the distribution.

The sum d of the divergences d_z corresponding to the various observables is computed and will be retained as the global divergence measuring to what extent we have to reject the Null Hypothesis for X^0 : the larger d , the higher our confidence level to reject the Null Hypothesis. If X^0 is in the acceptance interval (at 99%) for every and each observable, then d is simply zero and the Null Hypothesis is not rejected.

D. Final output of the constrained bootstrap method

The validity of the classical *unconstrained* bootstrapping relies on an unbiased randomness in the choice of the samples. In our case, by imposing constraints on the bootstrap samples, we lose some randomness and introduce possible dependencies: while the divergence d is sufficient to summarize an unconstrained test's outcome, we need here to also be especially careful to track the bias introduced by the constraints. In the following, we propose a practical way to control the validity of the procedure.

We track two indicators to monitor the bias introduced by constraints. The first one is the standard deviation σ_u of the distribution of the number of times each node is chosen in a bootstrap sample. It measures how uniformly a node is chosen in a bootstrap sample: the smaller is σ_u , the more the choice of the nodes for the bootstrap set is uniform. The second indicator measures if nodes in X^0 are chosen more – or less – often in the bootstrap samples than they would if there were no constraints. For that, we compare the empirical distribution of the number of nodes from X^0 that are in a bootstrap sample to the theoretical distribution valid if there were no constraint. This theoretical probability distribution of drawing k nodes from X^0 after $M = |X^0|$ draws without replacement in a total set of $V = |\mathcal{V}|$ nodes in the complete network is given by the hypergeometric law: $P(k) = \frac{\binom{M}{k} \binom{V-M}{M-k}}{\binom{V}{M}}$. We then compute the χ^2 distance between the empirical distribution and the theoretical hypergeometric distribution. In order to compare different χ^2 obtained from different bootstrap tests, each χ^2 value is computed with 10 bins that contain at

least five realisations. An important point is that we do not use χ^2 for a goodness-of-fit test. We indeed expect χ^2 to increase as soon as we impose stronger constraints on the bootstrap samples. Rather, we use χ^2 and σ_u as two control parameters of the “uniform character” of the bootstrapping procedure, and check that they stay reasonably small.

Finally, the output of the proposed test is a triplet (d, χ^2, σ_u) which summarizes the outcome of the test for X^0 . The larger is d , the higher the confidence level to reject the Null Hypothesis. The lower χ^2 and σ_u , the less biased is the choice of the pseudosamples and the more valid is the test.

IV. CASE STUDY: BOOTSTRAPPING UNDER CONSTRAINTS FOR SPECIFIC GROUPS OF ATTENDEES IN THE CONFERENCE

A. Choosing the groups and the Null Hypotheses

The original question of interest for the organizers of the SLC conferences is whether co-locating both conferences was worthwhile, i.e., whether the GEC and DPP communities mixed together. As previously shown, contacts did occur between individuals registered to the GEC and DPP. In order to give a quantitative answer to the question, one needs to compare the amount of interactions between GEC and DPP to some reference. In other words, are these interactions statistically significant? To answer such a question, the proposed bootstrap method is a natural candidate.

It is first important to note that the seven chosen observables that characterize a group’s “behavior” actually imply observables measured within the group (N_{XX} and T_{XX}), observables measured within the rest of the network (N_{RR} and T_{RR}), and observables measuring the interaction between the group and the rest of the network (N_{XR} , T_{XR} and Q_X). The terminology “group’s behavior” is used for simplicity, but the chosen observables quantify also the behavior of the group’s complementary as well as the interaction of the group with the rest of the network. Quantifying for instance “GEC’s behavior” represents therefore a possible measurement of the mixing between both communities, as the DPP individuals correspond precisely to the “rest” of the network. The method previously exposed is a means not only to quantify, but also to validate statistically, the normality – or abnormality – of GEC’s behavior with respect to various Null Hypotheses. We thus use this method for the group of GEC individuals, taken as the specific subset of interest X^0 in the face-to-face contact network between the attendees of the SLC conference.

The different Null Hypotheses that define the bootstrap samples X are taken as constraints on the amount of interaction involving nodes of X . We consider five different Null Hypotheses, or set of constraints: in each case, the Null Hypothesis can be phrased as “ X^0 has a behavior compatible with a random group X of nodes satisfying the chosen set of constraints”. We consider the following series of constraints on each random group:

- the size of the group is fixed, equal to the one of X^0 ;
- in addition, the modularity of the partition of the network between the group and its complement is equal to the one of the partition $(X^0, \mathcal{V} \setminus X^0)$;
- we will as well consider constraints on N_{XX} , T_{XX} or $T_{XX} + T_{XR}/2$, imposing that they take the same values as respectively $N_{X^0X^0}$, $T_{X^0X^0}$ or $T_{X^0X^0} + T_{X^0R^0}/2$, in addition to the size constraint. These constraints correspond to ways of imposing a certain number of links or a certain amount of interaction within the group, or between the group and the rest of the network.

We moreover consider the possibility that all groups with a community behavior (as given quantitatively by the seven observables) could appear as abnormal. We thus investigate the case of three other specific groups of individuals, that a priori could have a community behavior: the Students from DPP, i.e. attendants preparing a PhD thesis (STP), the Juniors from DPP, i.e. researchers with less than 10 years of professional experience (JUP), and the Seniors from DPP, i.e. researchers with more than 10 years of experience (SEP). Table II summarizes the measured observables for the GEC, STP, JUP and SEP. These groups can be considered a priori as communities because of similarities in age and professional status. We can therefore compare the tests’ outputs for GEC and for these other groups: if their behavior is similar, it could be argued that the subgroup GEC simply behaves as if it were a subcommunity of DPP, and the conclusion could be that the

Group	Cardinality	N_{XX}	N_{XR}	N_{RR}	T_{XX}	T_{XR}	T_{RR}	Q_X
GEC	39	101	120	1907	58820	45740	947100	0.100
STP	106	384	850	894	252900	356220	442540	0.145
JUP	73	183	766	1179	97600	303800	650260	0.073
SEP	99	226	704	1198	124280	310740	616640	0.095

TABLE II. The cardinality and the other seven observables of the four groups under study. The 3 time columns are in seconds.

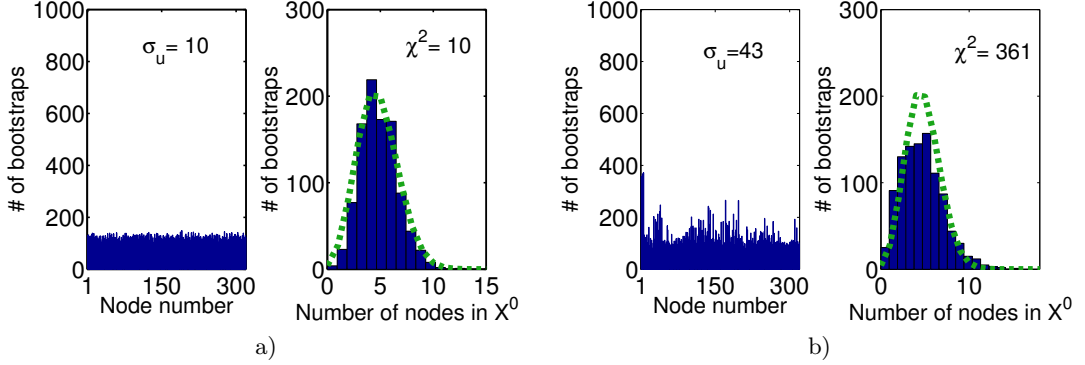


FIG. 3. Results for $X^0 = \text{GEC}$ for a) test with the same cardinality constraint, b) test with the constraints of same cardinality and same modularity ($\delta = 5\%$). Left: histogram of the number of occurrences of each node in the bootstrap samples and its standard deviation σ_u . Right: histogram of the number of X^0 -nodes in a bootstrap sample with its χ^2 distance from the theoretical hypergeometric histogram (dotted line).

co-location of the conference was an efficient way to bring together GEC and DPP. If instead GEC is significantly more abnormal than the three other groups, one may doubt the efficiency of the co-location.

Our approach is therefore to test those four groups (i.e., the group noted X^0 in the method will alternatively be GEC, STP, JUP, or SEP) against the same Null Hypotheses. We then compare the degree with which the Null Hypotheses are rejected for each group. In order to understand if GEC’s behavior is peculiar, we consider several Null Hypotheses, i.e., sets of constraints on the bootstrap samples, and investigate if they significantly discriminate GEC from the other groups.

We finally note that, in the following, the aggregated graph is pre-processed by deleting links between nodes that correspond to an aggregated contact time of the two corresponding individuals smaller than 1 minute over the whole conference. The threshold of 1 minute is chosen because smaller contact times can be considered as noise in the measurement, associated to very short contacts. We have checked that our results are robust with respect to the filtering threshold: similar results are obtained when thresholding at 3 and 5 minutes.

B. Cardinality constraint

We first consider the following simple Null Hypothesis: GEC behaves like any random group of $M = 39$ individuals in the conference. For this first Null Hypothesis, the only constraint we impose to the bootstrap samples is therefore to have a cardinality equal to M .

Applying the protocol described in III B, we first pick randomly $N_B = 1000$ bootstrap samples of 39 nodes. For each sample, we compute the seven associated observables and normalize them as proposed in III C. For each observable Z , the mean \bar{z}^b and the standard deviation σ_z^b are computed from the bootstrap samples: this defines what we call the “normal behavior” of a group under this constraint. We then obtain the divergences d_z for each feature, and finally the triplet (d, χ^2, σ_u) .

Figure 3.a displays two histograms, that show what the outputs σ_u and χ^2 aim at quantifying. On the left hand side, the histogram shows the number of times each node is chosen in the bootstrap

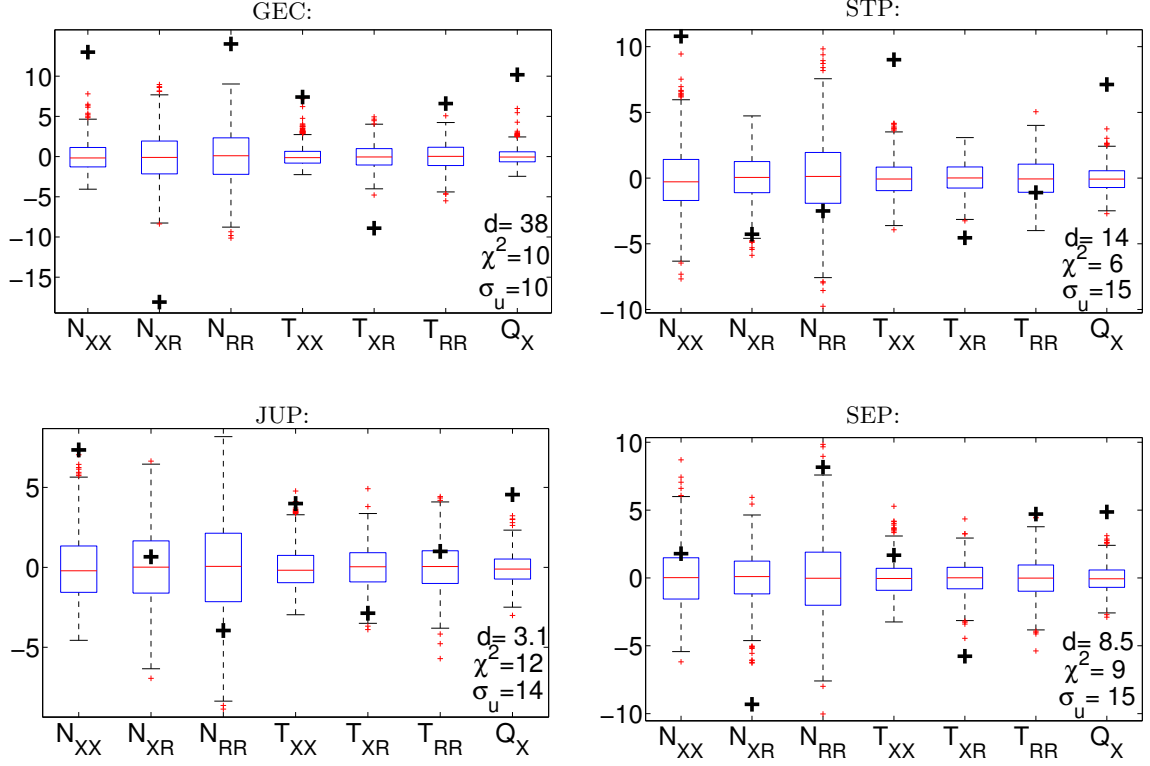


FIG. 4. Results of the test with same cardinality constraint. For each group $X^0 = \text{GEC, STP, JUP and SEP}$, the scalar d (bottom right hand corner of each figure) is an estimation of the distance between the statistical behavior of the bootstrap samples (boxplots) and the real data (big black crosses). χ^2 and σ_u are two control parameters of the “uniformity” of the test – see text.

set: the standard deviation σ_u quantifies whether the choice is uniformly random or not. On the right hand side, the distribution of the number of nodes of X^0 (GEC) chosen in each bootstrap sample is displayed: the χ^2 value measures the distance between the theoretical hypergeometric distribution and the actual one.

The top left plot of Figure 4 summarizes the output of this test for GEC: it compares for each feature the boxplots of the bootstrap samples with the measured behavior of GEC (black crosses) and gives the values of d , χ^2 and σ_u in the bottom right hand corner of the figure. The indicators χ^2 and σ_u are small: the bootstrap set and the test are valid; d is non-null: the Null Hypothesis is rejected. The other three plots of Figure 4 show the results for the three other groups (SEP, JUP, STP).

On each boxplot, the central red line is the median, the edges of the box are the 25th and 75th percentiles and the whiskers extend to the most extreme data points that are not considered as outliers. Points are drawn as outliers (small red crosses) if they are larger than $q_3 + w(q_3 - q_1)$ or smaller than $q_1 - w(q_3 - q_1)$, where q_1 and q_3 are the 25th and 75th percentiles, respectively. We use the value $w = 1.5$ which corresponds to approximately $\pm 2.7\sigma$ and 99.3% coverage if the data were normally distributed.

All 4 groups have a non-null divergence d and small χ^2 and σ_u : the Null Hypothesis is rejected for all. In other words, none of these groups of individuals behave similarly to a random group of nodes with the same cardinality. These results do not come as a surprise since, as previously mentioned, each of these groups are a priori communities and behave indeed as such: compared to the bootstrap samples, they tend to have larger Q_X , N_{XX} , N_{RR} , T_{XX} , T_{RR} and smaller N_{XR} , T_{XR} . Interestingly, GEC’s divergence is clearly larger than the others: this first test, even if somehow naïve, hints at some difference between GEC and the other groups.

C. More elaborate constraints

In order to better discriminate GEC's behavior from the behavior of other groups, we need to consider more refined Null Hypotheses, i.e., stronger constraints on the bootstrap samples. There is however a trade-off between the test's aptitude to be discriminative and too strong constraints that jeopardize the test's validity. Indeed, we expect χ^2 and σ_u to increase if we impose stronger constraints on the bootstrap samples. In the following, we explore cases that lie between extreme cases with large χ^2 and σ_u (invalidating the test), and the weak test performed in the previous paragraph, in which the only constraint is given by the cardinality. We explore this trade-off, making sure that the two control parameters χ^2 and σ_u stay small in order to obtain valid but discriminating tests (see Section IV E for a precise description of this trade-off).

We first consider the following refined Null Hypothesis, that takes into account the high modularity of X^0 : X^0 behaves like any random group of nodes with the same cardinality and the same modularity as X^0 (hence forming a community as strong as X^0). In fact, requiring the exact same modularity is too strong a constraint so that we relax it to: $Q_X^0(1 - \delta) \leq Q_X \leq Q_X^0(1 + \delta)$ with δ the error we tolerate. The value of δ tunes the strength of the constraint: the lower is δ , the stronger is the constraint (see section IV E). In the following, $\delta = 5\%$. The set of bootstrap samples is found using simulated annealing, as presented in Section III B. Figure 3.b shows the two same histograms as Figure 3.a, but for the bootstrap samples under this new constraint (for $X^0 = \text{GEC}$). As expected, they show a higher σ_u and χ^2 , yet not so large that the uniform character of the bootstrap samples would be questionable. The results for the four studied groups are summarized in Figure 5. First, we see that the boxplots are not centered around zero anymore, they indeed need to be in accordance with a high modularity (typically: high N_{XX} , T_{XX} and low N_{XR} and T_{XR}). Divergences are null for STP and JUP, while the divergence for SEP is almost ten times smaller than for GEC: this test shows that GEC's behavior is peculiar with respect to the other groups considered.

Other Null Hypotheses, implying other constraints can be considered: imposing $N_{XX} = N_{X^0X^0}$, imposing $T_{XX} = T_{X^0X^0}$, or $2T_{XX} + T_{XR} = 2T_{X^0X^0} + T_{X^0R^0}$. These constraints are ways to impose the amount of interactions involving nodes of each group, respectively in terms of numbers of contacts, of the cumulated duration of contacts inside the group, or of the duration of all contacts involving individuals in this group. Results are summarized in Fig. 6 for these three constraints (in each case, the cardinality constraint is as well imposed): the divergence from the bootstrap samples is always much larger for GEC than for the other groups. Note that each constraint (except the cardinality constraint) is relaxed in the same way as the modularity constraint with $\delta = 5\%$.

Even though the modularity constraint is the most successful in discriminating GEC from the three other groups, the three other tests show corroborative evidence of GEC's peculiar behavior. The outputs of all the different tests are consistent, and they show not only that GEC behaves in a peculiar fashion, but also in what ways GEC behaves differently. For instance, under the constraint of fixed modularity, the boxplots for GEC show that it has particularly high N_{XX} , N_{RR} , T_{RR} while having very low N_{XR} , T_{XR} and slightly low T_{XX} features as compared to random groups of nodes with the same modularity: the precise reasons for the rejection of the Null Hypothesis are highlighted.

D. Different locations

As discussed in Section II and exhibited by the distribution of the contact durations measured in the different areas of the conference, some spatial heterogeneity is observed in the data. We take advantage of the coarse localization of the contacts to investigate the effect of the location on the behavior of the groups. To this aim, we perform separate tests on the data collected in the three different areas: *the GEC area*, *the Poster Hall* and *the Rest*. Results are presented in Fig. 7. The test clearly differentiates GEC's behavior from the others' in all areas. However, the difference in behaviors (and the divergence obtained with the GEC group) is smaller when measured in the Poster Hall or in the "Rest" of the conference. This result has a simple interpretation: first, GEC mixed significantly more with DPP in the areas that were actually common to both conferences; second, the members of GEC who went to the location of the DPP conference mixed indeed with DPP. This leads us to a somehow obvious remark: organizing activities in common physical spaces favors the mixing between two communities.

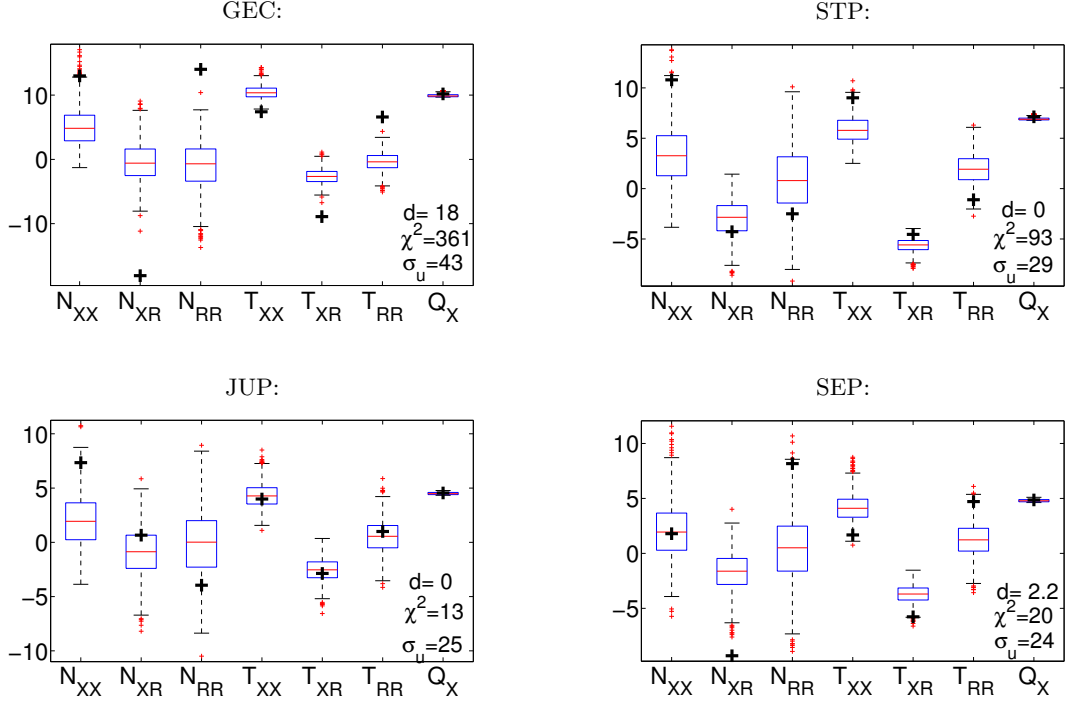


FIG. 5. Results of the test with the constraints of fixed cardinality and fixed modularity ($\delta = 5\%$) for the four groups.

Null Hypothesis	GEC	STP	JUP	SEP
Fixed cardinality constraint	(38, 10, 10)	(14, 6, 15)	(3.1, 12, 14)	(8.5, 9, 15)
Fixed cardinality and N_{XX} constraint	(68, 1876, 96)	(14, 236, 98)	(2, 84, 69)	(19, 7, 23)
Fixed cardinality and T_{XX} constraint	(32, 165, 63)	(4, 804, 121)	(0, 9, 53)	(15, 20, 31)
Fixed cardinality and $T_{XX} + \frac{T_{XR}}{2}$ constraint	(46, 156, 49)	(12, 237, 70)	(5, 8, 16)	(9, 25, 43)
Fixed cardinality and Q_X constraint	(18, 361, 43)	(0, 93, 29)	(0, 13, 25)	(2.2, 20, 24)

FIG. 6. Summarized results for various sets of constraints. Each entry of the table represents the triplet (d, χ^2, σ_u). All constraints except the cardinality constraint are relaxed with $\delta = 5\%$.

E. Trade-off between the constraint(s) strength and the validity of the test

We focus on the trade-off between the constraints' strength and the validity of the test. Strong constraints make χ^2 and σ_u increase, but until now, we did not specify what we mean by “too large” for these two indicators (i.e. what we mean by “too strong” for a constraint). We focus on this question in the following.

As mentioned previously, the parameter δ enables us to tune the “strength” of a given constraint: the lower is δ , the stronger the constraint. The trade-off is between a small δ that ensures that the bootstraps keep the wanted correlations but that reduces the space of possible bootstraps hence jeopardizing the observables' statistics, and a large δ that ensures a large space of possible bootstraps but that creates bootstraps with less correlations. There is an analogy between this discussion and the one on the optimal size l^* of the blocks in block bootstrapping [21, 22] ($\frac{1}{\delta}$ is analogous to l). With Monte Carlo methods, we could try to estimate the reduction of the space of possible bootstraps due to a strong constraint. This is intractable in our case where the space of possibilities is huge (there are C_n^k groups of k nodes in a set of n nodes) and where the reduction of space due to a constraint is possibly drastic. We instead use χ^2 and σ_u as two indirect measures of this reduction of space. Indeed, in the extreme case where we impose the bootstrap samples to be exactly the X^0 group by using too strong constraints (the size of the space of possible bootstraps

Null Hypothesis	area	GEC	STP	JUP	SEP
Same cardinality constraint	GEC area	(96, 9, 10)	(14, 16, 16)	(1, 4, 14)	(0, 17, 14)
	Poster Hall	(12, 11, 10)	(9, 16, 15)	(1, 2, 13)	(2, 13, 14)
	The Rest	(9, 6, 10)	(11, 8, 15)	(5, 10, 13)	(9, 13, 15)
Same cardinality and same modularity constraint	GEC area	(80, 1144, 32)	(10, 12, 22)	(1, 12, 21)	(0, 6, 19)
	Poster Hall	(11, 32, 19)	(2, 25, 24)	(0, 11, 18)	(1, 5, 15)
	The Rest	(7, 6, 11)	(0, 65, 28)	(0, 30, 29)	(0, 49, 30)

FIG. 7. Results for the tests with fixed cardinality constraint and fixed cardinality and modularity constraints for the different locations within the conference. Each entry of the table represents the triplet (d, χ^2, σ_u) .

is here reduced to one), σ_u is larger than 300, and χ^2 larger than 10^{48} (the expected number of bootstrap samples having 39 nodes is $P(V) \times N \sim 10^{-48}$). In some sense, the simulated annealing procedure acts as a biased Monte Carlo estimation of the size of the reduced space of possible bootstraps.

Given a confidence level α for the test to be valid, it would be very valuable to formally obtain thresholds χ^{2*} and σ_u^* under which the space of possible bootstraps is large enough and the test thereby considered valid. Unfortunately, even in the easier case of block bootstrapping, automatic estimation of the optimal size l^* has only been obtained for specific estimators and the general question remains open.

These thresholds χ^{2*} and σ_u^* in turn give a threshold value δ^* that represents the trade-off we are looking for. In Fig. 8, we plot the evolution of the results of the test (d, χ^2, σ_u) with respect to δ for the four groups. Fig. 8a is for the same cardinality constraint and the same N_{XX} constraint and Fig. 8b for the same cardinality constraint and the same T_{XX} constraint. Naturally, χ^2 and σ_u decrease with δ as the constraint is gradually relaxed, until it converges towards the triplets obtained with the same cardinality constraint. As we do not have an analytical link between a confidence level α and the values of the threshold, we are bound to give them from empirical observation: we propose $\chi^{2*} = 1000$ and $\sigma_u^* = 80$. Fig. 3.b shows two histograms that are considered acceptable ($\chi^2 < \chi^{2*}$ and $\sigma_u < \sigma_u^*$). Fig 17 in the annex shows two histograms that are considered unacceptable. δ^* is defined for a given constraint, a given graph, and a given subgroup X^0 . If we want to compare the output for four different X^0 groups for a given constraint, we need to choose the largest δ^* out of the four.

Looking at Fig. 8, we obtain $\delta^* = 20\%$ for the N_{XX} constraint; and $\delta^* = 25\%$ for the T_{XX} constraint. We do not show the results for the other two constraints, but we estimated $\delta^* = 3\%$ for the $2 \times T_{XX} + T_{XR}$ constraint; and $\delta^* = 0.001\%$ for the modularity constraint.

V. THE CASE OF WEIGHTED RANDOM GRAPHS

In this section, we test our methodology in a controlled setting. We investigate if the proposed test can distinguish between a large random fluctuation of behavior – which is rare but can still be considered as “normal” – and a truly abnormal behavior. To address this issue, we apply the method to a specific type of network which follows a usual model of complex network, the so-called Chung-Lu model [13]: this model produces random networks with a pre-defined distribution of degrees. In the following, we first adapt this model to weighted graphs, before presenting our results.

A. Weighted Chung-Lu graphs

A Chung-Lu graph [13, 23] is a random graph with a given expected degree sequence. Consider $(k_i)_{i=1, \dots, V}$ the expected degree sequence and $W = \frac{1}{2} \sum_i k_i$ the expected total number of edges. In a Chung-Lu graph, the probability that a given edge (connecting nodes i and j) exists is given by $\min(1, \frac{k_i k_j}{2W})$.

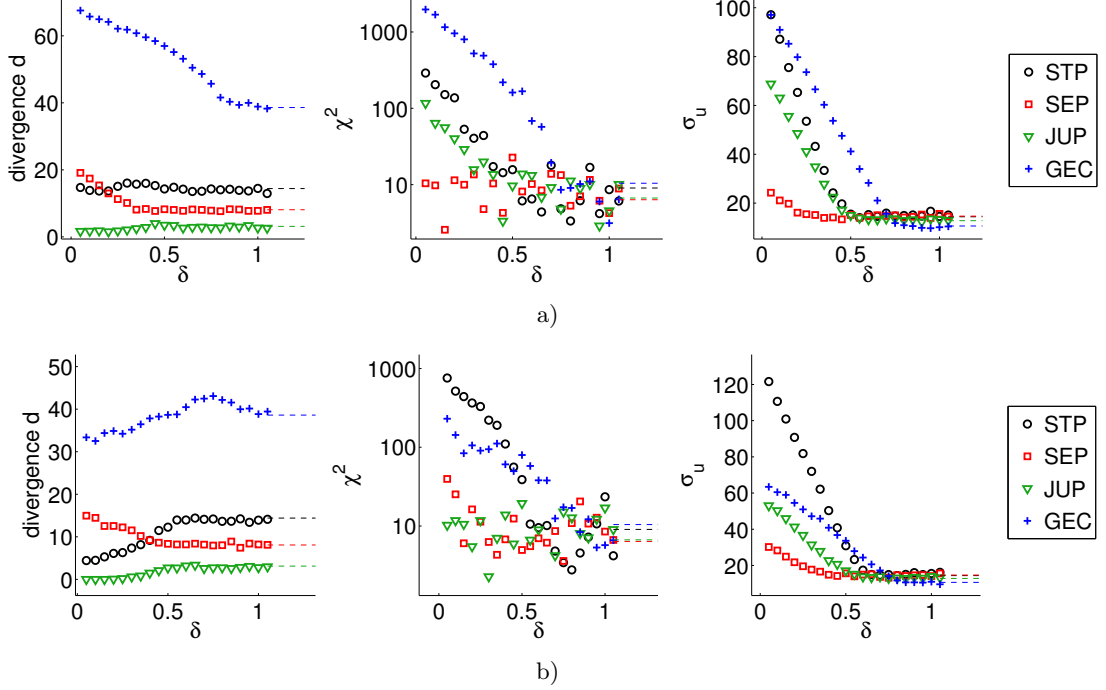


FIG. 8. Evolution of the triplet (d, χ^2, σ_u) with the constraints of (a) fixed cardinality and fixed total number of internal links (N_{XX}) and (b) fixed cardinality and fixed total time of contact T_{XX} , with respect to δ for the four groups. We observe a convergence towards the fixed cardinality constraint results (dashed horizontal lines).

As we are interested here in weighted networks, we first introduce a model of weighted Chung-Lu graph: to this aim, we create a non-weighted (or binary) Chung-Lu graph, and allocate a weight to each edge. In real networks, weights and topology are often not independent [24]. This is the case in the networks of face-to-face contacts considered previously, as shown in Fig. 9, that displays the average strength of nodes as a function of their degree (we recall that the strength of a node is the sum of the weights of its edges). In order to produce random weighted networks exhibiting similar correlations, we compute from the real data, for each degree k , the empirical distribution of the weights of the links attached to nodes of degree k . We model each of these distributions by a power law to obtain an estimated distribution $P_k(w)$ [25]. A weighted Chung-Lu graph is thus built in the following way: we start by creating a binary Chung-Lu graph with the same expected degree sequence as the data. For each node i (of degree k_i) of this Chung-Lu graph, we draw weights from the appropriate distribution P_{k_i} and randomly allocate them to its links whose weight has not yet been specified (if i is linked to a node j that has already been considered, then the weight of link $i - j$ has already been chosen by using P_{k_j} and it does not need to be computed again). In this way, the weight sequence will be similar to the empirical graph's, if not exactly the same. We thereby obtain a weighted Chung-Lu graph with the same expected degree sequence, the same strength-degree correlation and a similar weight sequence than the empirical graph. Figure 9 shows in particular that the strength-degree correlation of such a weighted Chung-Lu graph is in agreement with the empirical data. Each Chung-Lu graph we generate can be seen as a topologically randomised version of the graph of contacts we measured.

Note that this randomisation is in no way related to the one proposed for the bootstrap samples. Hence, it is possible to use these weighted Chung-Lu graphs as a controlled input to test the method.

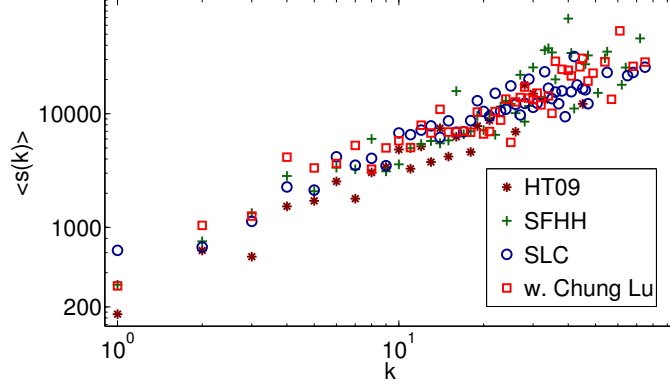


FIG. 9. Average strength versus degree of nodes in three different scientific conferences. The squares represent the same quantity for a weighted Chung Lu graph generated from the empirical distributions of the SLC contact network.

B. Groups' modularity in weighted Chung-Lu graphs

Let us consider random groups of nodes, of cardinality $M = 39$ (like GEC) and study their modularity in weighted Chung Lu graphs. Figure 10.a) reports the histogram of the modularity of such randomly drawn groups. The histogram was obtained by computing 500 different realisations of weighted Chung-Lu graphs and measuring, for each realisation, the modularity of 1000 groups of 39 nodes.

Figure 10b) shows the histogram of the maximum modularity found in a weighted Chung-Lu graph. This second histogram was obtained by looking for a group (of cardinality 39) of maximum modularity in 740 different Chung-Lu graphs using simulated annealing. Because the number of possible groups of 39 nodes is huge, this histogram is only an estimation of the maximum modularity: we stop the simulated annealing search after an arbitrary amount of time without new result. Interestingly, this histogram seems to fit a Weibull distribution, the extreme values distribution in the case of the existence of an upper bound. The χ^2 goodness-of-fit test fails (with a p-value of 10^{-5}) but this could be accounted for by the fact that we only have an estimation of the extremal value. In fact, we expect a Weibull distribution for independent identically distributed random variables having an upper bound, like modularity.

C. Proposing a controlled model

Let us insist on an important distinction that is at the heart of our discussion: the difference between rare and abnormal events. For instance, in these Chung-Lu graphs, an overwhelming majority of groups have modularity lower than 0.08 (out of half a million random tries, none had a modularity higher than 0.08). We can therefore affirm that a group with a modularity of, say, 0.16 is rare, however it is not necessarily abnormal. If it is not *too* rare (which translates, in the bootstrap approach, to : if σ_u and χ^2 are not too high), then we have enough bootstrap samples to compare it with, and we are able to test whether or not it is abnormal with respect to other groups with the same modularity. If it is too rare (i.e. if σ_u and χ^2 are too high), then we do not have enough statistics and we are unable to conclude.

For each generated weighted Chung-Lu graph, we choose 10 groups with modularities incremented from 0 (the most common) to 0.18 (the rarest). We apply the method to each of these groups (X^0 being alternatively each of these 10 groups), and we repeat on a large number of Chung-Lu graphs to obtain the average performance of the method. We use four different Null Hypotheses for the bootstrap tests, corresponding to: i) the fixed cardinality constraint (“Card”), ii) the constraints of fixed cardinality and total number of links within the group (“ N_{XX} ”), iii) the constraint of fixed cardinality and total time of interaction within the group (“ T_{XX} ”), and iv) the constraint of fixed cardinality and modularity (“Modu”). As the graphs are random, all groups

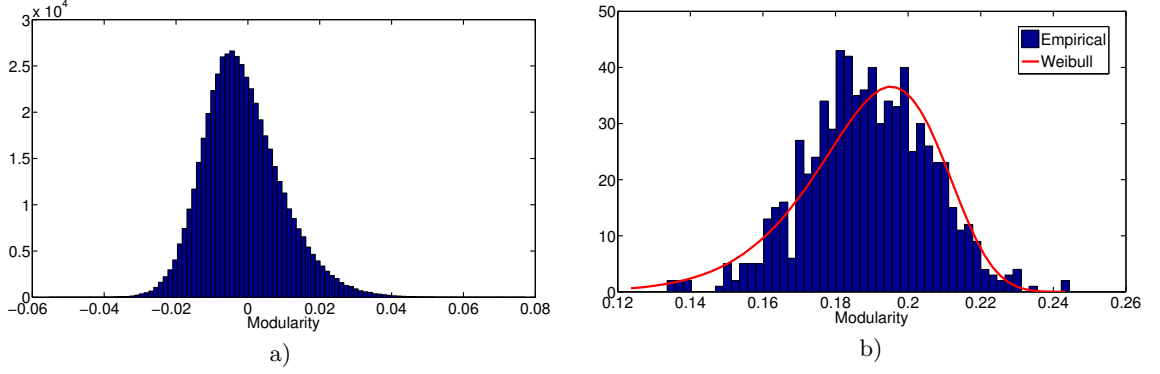


FIG. 10. a) Histogram of the modularity of a sub-graph of 39 nodes in a weighted Chung-Lu graph and b) Histogram of the estimated maximal modularity of a group of 39 nodes in a weighted Chung-Lu graph. This histogram is fitted with a Weibull distribution.

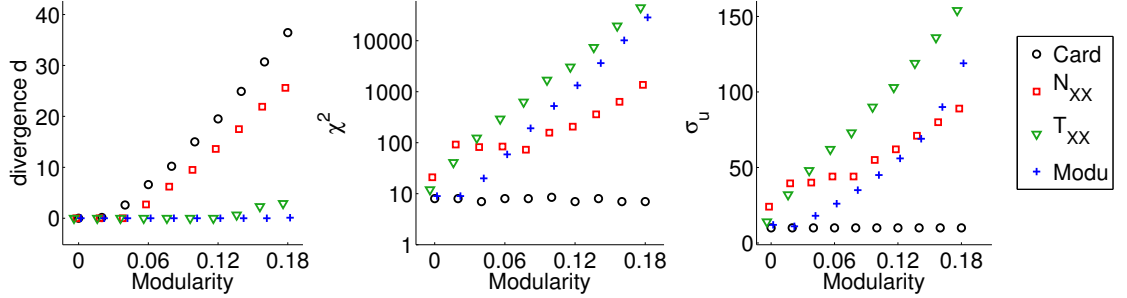


FIG. 11. Median performance of the method with respect to the “rarity” of a group (here quantified by its modularity) on the weighted Chung-Lu model.

(whether common or rare) are somehow “normal”, and, in average, should be classified as such by the method.

An important remark is that we choose here to quantify the “rarity” of a group with respect to its modularity, and then test how well the tests differentiate rare groups from abnormal ones. This choice of definition for the rarity of a group has of course an impact on the performances of the tests. We could have chosen to quantify the rarity with respect to other features, such as N_{XX} for instance. Our purpose here is however not to test the methodology on an exhaustive list of controlled models, but rather to illustrate a way to test the methodology with a given definition of rarity.

D. Results of bootstrap tests on groups in weighted Chung-Lu networks

We test the method on 240 weighted random Chung-Lu graphs and show the median of the outputs (d, χ^2, σ_u) in Fig. 11, as a function of the modularity of the studied groups.

E. Interpretation

As expected, χ^2 and σ_u increase monotonically with the rarity of the considered groups (the higher the modularity, the rarer the groups). Following the discussion of IV E, we define a “threshold of uniformity” beyond which the test is considered untrustworthy: if χ^2 is larger than $\chi^{2*} = 1000$ and/or σ_u larger than $\sigma_u^* = 80$, the output of the method is that no conclusion can be drawn because the considered group is too rare.

In this context, the modularity constraint test has a very good performance: it correctly classifies the groups as normal for modularities under 0.12 and classifies the groups as too rare beyond. It never misclassifies groups as abnormal. Interestingly, even though the observable T_{XX} is not obviously correlated to the modularity, the T_{XX} constraint test also performs well: it correctly classifies the groups as normal for modularities under 0.08 and classifies the groups as too rare beyond; and it never misclassifies groups as abnormal. On the other hand, the cardinality (resp. N_{XX}) constraint test performs poorly. It never classifies the groups as too rare to give an answer, and starts to misclassify groups as abnormal from a modularity of 0.02 (resp. 0.04). This does not come as a surprise. In fact, we have seen that the concept of “normality” is defined with respect to a Null Hypothesis. We see here that “normality” with respect to the modularity is not the same as the “normality” with respect to N_{XX} . More specifically, a rare group (with respect to modularity) is detected as abnormal with respect to N_{XX} .

The modularity of GEC in the SLC conference dataset is 0.10. We can not exactly compare this modularity with the modularities of random groups of weighted Chung Lu graphs because the empirical network has a well-defined structure that is different from a random Chung Lu graph. The order of magnitude is however relevant and lies in the validity region of the test. The conclusion of this section is that the bootstrap approach presented to test normality of groups in the conference dataset is appropriate and does not inappropriately classify groups as abnormal.

VI. CONCLUSION

We have proposed in this work a generic method to compare the behavior of specific groups of nodes within a given weighted complex network. The method is inherently flexible: depending on the issue addressed in the data at hand, some observables and Null Hypotheses will be more appropriate than others. We show via the construction of a controlled model that our method is robust with respect to random fluctuations of behavior and that it is able to distinguish a rare behavior from a truly abnormal one. We have shown on a new dataset of time-resolved, face-to-face human contacts collected during two co-located conferences, that the smaller conference was indeed seen as an abnormal group in a statistically significant way. It has fewer contact numbers and interaction durations with people from the other conference, even when accounting for its organization as a community of high modularity. Another finding was that the mixing was better in spaces that were shared by the two conferences.

More generally, the proposed method for bootstrapping and statistical test in complex network can be used in a larger setting: it can be applied to any type of data that can be modelled by graphs. Future work includes applying this method for data collected at various times of the day. Another development would be to propose Null Hypotheses that directly involve the dynamic behavior of groups and not only their aggregated behavior over time.

ACKNOWLEDGMENTS

We thank the SocioPatterns collaboration [14] for providing privileged access to the SocioPatterns sensing platform that was used in collecting the contact data. A.B. is partially supported by FET project MULTIPLEX 317532. This work has been supported by the CNRS (PEPS “ARDyC”, 2011).

-
- [1] C. Cattuto, W. Van den Broeck, A. Barrat, V. Colizza, J. Pinton, and A. Vespignani, *PloS one* **5**, e11596 (2010).
 - [2] N. Eagle and A. Pentland, *Personal and Ubiquitous Computing* **10**, 255 (2006).
 - [3] P. Hui, A. Chaintreau, J. Scott, R. Gass, J. Crowcroft, and C. Diot, in *Proceedings of the 2005 ACM SIGCOMM workshop on Delay-tolerant networking* (ACM, 2005) pp. 244–251.
 - [4] M. Salathé, M. Kazandjieva, J. Lee, P. Levis, M. Feldman, and J. Jones, *Proceedings of the National Academy of Sciences* **107**, 22020 (2010).
 - [5] A. Drummond and A. Rambaut, *BMC evolutionary biology* **7**, 214 (2007).

- [6] N. Friedman, M. Goldszmidt, and A. Wyner, in *Proceedings of the Fifteenth conference on Uncertainty in artificial intelligence* (Morgan Kaufmann Publishers Inc., 1999) pp. 196–205.
- [7] S. Fortunato, *Physics Reports* **486**, 75 (2010).
- [8] A. Lancichinetti, F. Radicchi, and J. J. Ramasco, *Phys. Rev. E* **81**, 046110 (2010).
- [9] B. Efron, *The jackknife, the bootstrap, and other resampling plans*, Vol. 38 (Society for Industrial and Applied Mathematics Philadelphia, 1982).
- [10] A. Zoubir and D. Iskander, *Bootstrap techniques for signal processing* (Cambridge University Press, 2004).
- [11] H. Eldardiry and J. Neville, in *Proceedings of the 2nd SNA Workshop, 14th ACM SIGKDD Conference on Knowledge Discovery and Data Mining* (2008).
- [12] X. Ying and X. Wu, in *Proc. of the 9th SIAM Conference on Data Mining* (2009).
- [13] F. Chung and L. Lu, *Proceedings of the National Academy of Sciences* **99**, 15879 (2002).
- [14] www.sociopatterns.org, .
- [15] L. Isella, J. Stehlé, A. Barrat, C. Cattuto, J. Pinton, and W. Van den Broeck, *Journal of theoretical biology* **271**, 166 (2011).
- [16] S. Lahiri, *The Annals of Statistics* **27**, 386 (1999).
- [17] D. Politis, *Statistical Science* **18**, 219 (2003).
- [18] M. Newman, *Physical Review E* **70**, 056131 (2004).
- [19] S. P. Brooks and B. J. T. Morgan, *Journal of the Royal Statistical Society. Series D (The Statistician)* **44**, pp. 241 (1995).
- [20] We have checked that the distributions of the 7 considered observables are close to being Gaussian distributed; in fact, some fit Gaussian distributions, others fit Gamma distributions, but none displays heavy-tailed distributions, so that the mean and standard deviation are well-defined.
- [21] P. Hall, J. Horowitz, and B. Jing, *Biometrika* **82**, 561 (1995).
- [22] P. Bühlmann and H. Künsch, *Computational Statistics & Data Analysis* **31**, 295 (1999).
- [23] J. Miller and A. Hagberg, *Algorithms and Models for the Web Graph* , 115 (2011).
- [24] A. Barrat, M. Barthélemy, R. Pastor-Satorras, and A. Vespignani, *Proc. Natl. Acad. Sci. (USA)* **101**, 3747 (2004).
- [25] If there are not enough nodes of degree k in the original data to obtain a reasonable fit, we use the 50 nodes whose degrees are closest to k to compute $P_k(w)$.

ANNEX

A. Map

Figure 12 shows the map of the conference venue in Salt Lake City. GEC was situated around antennas 20 and 21: very far from the rest.

B. Comparison between three conferences

The social interactions measured in all three conferences (HTT09, SFHH and SLC) show similar distributions. For instance, Figure 13 shows the distribution of the duration of intercontacts. The distribution of degrees is shown in Fig. 14 and the distribution of the weights of the links in Fig. 15. Finally the property of small world is shown in Fig. 16.

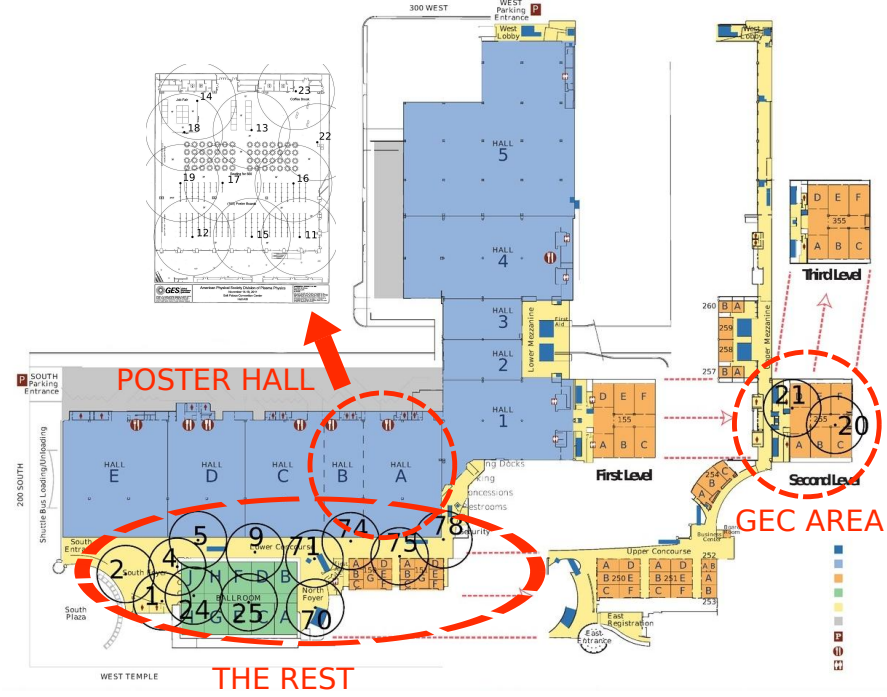


FIG. 12. General map of the conference venue with the three different general areas. Each black circle corresponds to one of the 25 antennas used to measure the social interactions. The GEC area is isolated: it is 500 meters away from the Poster Hall.

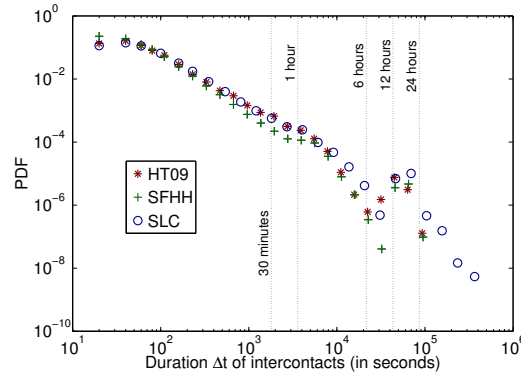


FIG. 13. Distribution of the duration of intercontact: duration of the time, for a node, between two starts of contacts.

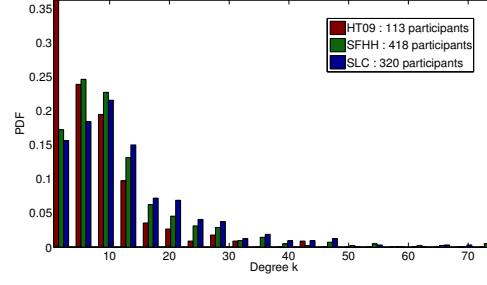


FIG. 14. Distribution of degrees.

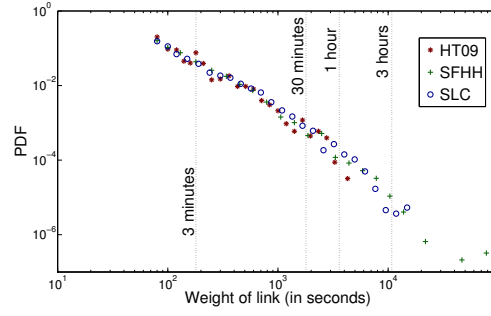


FIG. 15. Distribution of weights of the links.

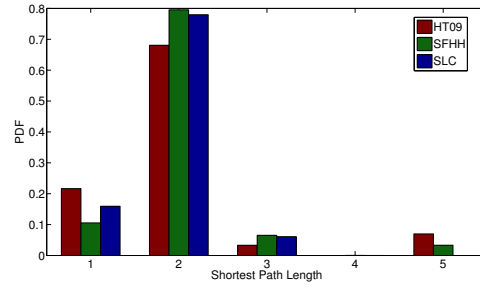
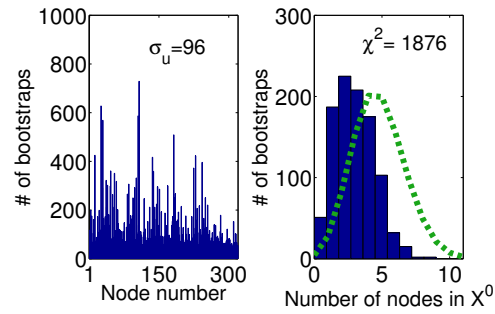


FIG. 16. Histogram of the shortest paths' length. It shows the property of small world.

FIG. 17. Example of a constraint considered as too strong: the same cardinality constraint and the same total number of internal links (N_{XX}) with $\delta = 5\%$ for $X^0 = \text{GEC}$.